HNPS Advances in Nuclear Physics

Vol 5 (1994)

HNPS1994

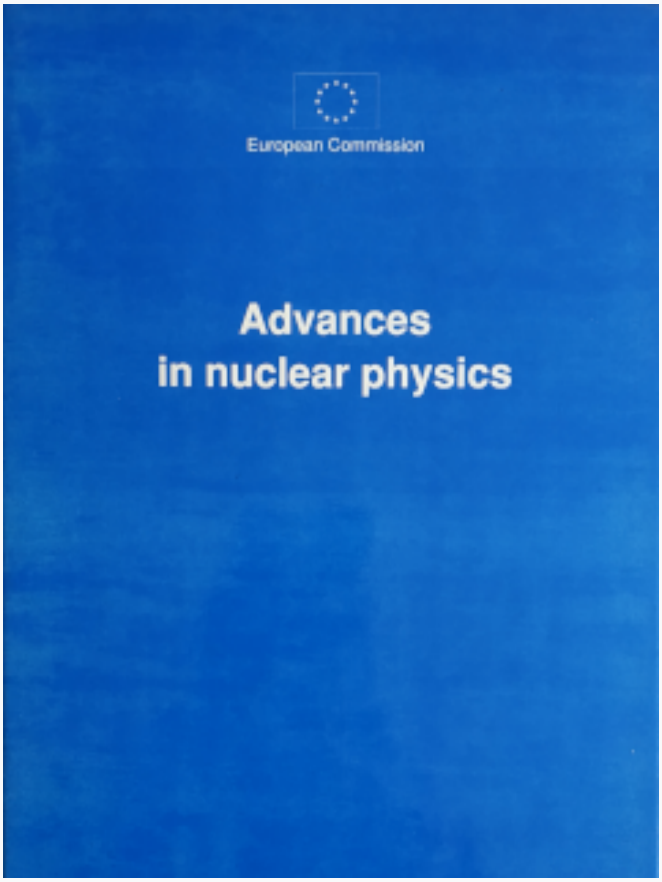

Recent Developments in High Temperature Thermodynamic Properties of Nuclear Reactor Oxide Fuel

C. Ronchi

doi: 10.12681/hnps.2909

RECENT DEVELOPMENTS IN HIGH TEMPERATURE THERMODYNAMIC PROPERTIES OF NUCLEAR REACTOR OXIDE FUEL

C.Ronchi

European Commission
Joint Research Centre
European Institute for Transuranium Elements
Karlsruhe, Germany

INTRODUCTION

During the last decade an effort was made in the principal nuclear research laboratories in Europe and U.S.A. aimed at defining the thermohydraulic and thermodynamic behavior of the degraded Liquid Metal Fast Breeder Reactor (LMFBR) core under accident conditions. The most severe hypothetical accident in this type of ractor is triggered by simultaneous failure of the operation and emergency cooling systems, which, after producing sodium boiling and voidance, may finally lead to self-enhanced prompt reactivity excursions occurring within a time interval as short as few milliseconds. The integral fission energy deposited during the reactivity ramp, and hence the further development of the hypothetical accident, is determined in this very short time during which the only reactor feedback is the thermodynamic adiabatic response of the core. In the worst cases, when core melt-down cannot be prevented, the only limiting factor for the total released energy is the early disassembly of the core under the thrust of the inner pressures, which, under the most conservative conditions, are provided by the equilibrium vapor pressure of the fuel mass.

In-pile experiments were carried out with the specific objective of determining the thermodynamic equation of state of the fuel in the fluid state (SANDIA-EOS, HARWELL-VIPER, CEA-SILENE), as well as laboratory measurements of selected thermodynamic properties of UO_2 at very high temperatures (ITU-Karlsruhe, KfK, ANL). Yet, the closure of most of the LMFBR development projects at the end of the 80's entailed the premature termination of these studies. However, more recently, in a reactor safety scenario open to wider perspectives, a new interest is raising in the fuel behavior under extreme temperatures conditions. The problem was presently resumed with the purpose of formulating a validated general theory of the equation of state of uranium dioxide both in the solid and liquid state.

This paper presents a review of the experimental data obtained during the last years and discusses the ruling thermophysical mechanisms in the oxide fuel at very high temperatures.

RELEVANT HIGH TEMPERATURE PROPERTIES OF UO_2

1) Heat Capacity of the Solid

This is a primary quantity, both from the technological (it governs the pile energy-temperature conversion) and physical (it represents the effective energy exchanges mechanisms) point of view. The function $C_p(T)$ was recently experimentally determined by calorimetric measurements in a laser-heated high-pressure autoclave [1] [2]in solid and liquid UO_2 (Fig.1). The empirical curve can be subdivided into distinct segments, corresponding to the elementary mechanisms operating at different temperatures:

The shape of the segment between RT and 1500 K is characteristic for most simple solids and is attributed to the activation and saturation of the harmonic lattice vibrations. Additional contributions are also present due to anharmonic vibrations (a temperature-linear term) and to crystal field transitions (an almost constant term).

From 1500 K to 2670 K ($= T_t$) the additional increase in C_p is caused by formation of lattice and electronic defects. The peak of C_p measured at $T_t \simeq 0.8 T_m$ (which indicates a sharp thermodynamic transition) is very similar to that observed in some ionic fluorides which exhibit a superionic λ –transition. Following ref. [3], this transition is interpreted as a critical phenomenon produced by *cooperative* creation of defects in the sublattice of the more mobile atomic species of type:

$$O_{lattice} \rightarrow O_{interstitial} + O_{vacancy} \qquad (1)$$

leading to a sudden increase in the oxygen vacancy/interstitial (*anti-Frenkel*) pair concentration at a defined critical temperature, T_t [4]. This interpretation is corroborated by neutron scattering measurements of the oxygen defect concentration n as a function of temperature [5], whose curve shows a steep inflection point at $T = T_t$.

Moreover, the d.c. electrical conductivity of UO_2 sharply increases in this temperature interval due to creation of electronic defects [6], entailing a further contribution to the heat capacity.

From T_t to T_m the function $C_p(T)$ is characterized by a steep descending flank of the λ –transition peak, due to the rapid saturation of the defect concentration after formation of an anion-disordered phase, followed by a weakly increasing stage due to the onset of the creation of more energetic atomic defects (UO_2 – neutral *Schottky* trios) whose sudden increase at the melting point represents the distinctive feature of the transition from the solid to the liquid phase.

In the liquid, from T_m to 4500 K the heat capacity decreases near to the level attained in the solid at 1500 K, indicating that all thermally activated processes are saturated on melting, leaving only atomic vibrations to support further heat exchanges.

At very high temperatures, from 4500 K to 8000 K a C_p upswing is observed due to more energetic electron excitations.

From this brief overview of the elementary mechanisms contributing to the heat capacity of UO_2 one realizes that the central problem for a comprehensive microscopic model of the system is the description of the atomic and electronic defect behavior, which governs the thermodynamic properties of the solid fuel at high temperatures.

2) The Pre-melting λ – Transition

This kind of transition generally occurs in polyatomic crystals where one atomic species has a higher sublattice mobility and a lower thermal stability than the other sublattices which, on the other side, are able to maintain their crystallographic configurations even in the presence of a large disorder in the sublattice of the more mobile species. For instance, in a class of halides (e.g. $SrCl_2$, BaF_2, PbF_2) at $T \simeq 0.8 T_m$ the ionic conductivity increases abruptly due to a steep substantial raise in the lattice defect concentration. The configurational entropy increase across this critical temperature is so large that one can see this transition as a forerunner of melting, whence the *pre-melting* appellation.

The pre-melting transition in UO_2 was first discovered by the analysis of the temperature derivative of the empirical enthalpy curve $H = H(T)$, and was later investigated in more detail by using a dynamic calorimetric method (thermal arrest by cooling) in both stoichiometric and off-stoichiometric $UO_{2\pm x}$ [2] (see Fig. 2a,b).

Interestingly, the transition gradually disappears in increasingly hyperstoichiometric UO_{2+x}, whilst in the hypostoichiometric oxide it assumes a clear first-order character, with a transition temperature increasing with x. Therefore, in the oxygen deficient solid solution UO_{2-x} two phases are respectively formed below T_t (oxygen ordered phase) and above T_t (oxygen disordered phase), whilst in UO_{2+x} anion disorder increases with temperature without solution of continuity. In the stoichiometric oxide a second-order transition is observed, where, by definition, the defect concentration $n(T)$ is a continuous and regular function of temperature, but at a critical temperature is $dn/dT = \infty$. Finally, the oxygen order/disorder transition exhibits a continuous evolution across the phase domain of the solid solution $UO_{2\pm x}$, passing from a 1st-order character in the range $O/U < 2$ to a 2nd-order at $O/U = 2$, and to a continuous increase of defect concentration with temperature for $O/U > 2$.

The pre-melting transition is caused by synergistic forces assisting the formation of oxygen defects (*Frenkel* interstitial/vacancy pairs), whereby the enthalpy of formation of one defect is a decreasing function of the defect concentration, owing to a second-order term of rank $\prec n^2$ which accounts for the attraction of complementary defects. In simple words, the more defects are present in the lattice, the less mechanical work is needed to create one additional defect; at the limit, this work may become so small that any further increase in defect concentration, e.g. by increasing temperature, affects the free energy only through the entropy variation. Therefore, it is not surprising that, under these conditions, the system tends to reach the state of maximum disorder attainable in the given configurational space of the crystal.

Since the predominant acting forces in the UO_2 lattice are of Coulombic type, the interaction between defects was analyzed with different models based on mean-field electrostatic screening (typically based on *Debye-Hückel's* approximation), where the defect free energy is generally written as:

$$\Delta G(n,T) = n\Delta H_0 + \Psi(n,T) - nT\Delta S(n) \tag{2}$$

where ΔH_0 is the defect enthalpy of formation *at zero defect concentration*, whilst the function Ψ depends on the defect intersite screening potential (i.e. a negative or "attractive" term). In our case Ψ was given different forms, from the classical *Hückel* approximant to simpler phenomenological linear expressions. The thermodynamic equilibrium conditions are given by the defect concentration n which satisfies the equation:

$$\frac{\partial \Delta G(n,T)}{\partial n} = 0 \tag{3}$$

Since ΔS, the defect entropy, can be deduced from the UO_2 crystal lattice configuration[1] and from the effective perturbations of the vibration frequencies around the defect, the properties of the solutions of eq.(3) were investigated in the stoichiometric and off-stoichiometric uranium oxyde.

The relevant results of this analysis can be summarized as follows:

1. If the UO_2 *mean-field* dielectric properties (the effective ionic radii and the static dielectric constant, which in UO_2 is $D = 24 \pm 4$) are used to calculate Ψ (e.g. with the *Debye-Hückel* approximation), eq.(3) is able to predicts a second-order transition at 2670 K for the stoichiometric oxide (Fig.3 a and b).

---

1 The experiment shows that oxygen defects in UO_2 are arranged in clusters, which at high temperatures mainly consist of two ajacent vacancies surrounded by 3 or 4 interstitials occupying strained lattice positions. Clustering is accounted for in the expression of the configurational part of ΔS.

2. If the absolute stoichiometric deviation, x, is accounted for in the entropy terms, ΔS, the solutions of eq.(3) are conform to the experimental results, with a predicted first-order transition in UO_{2-x} and no transition in UO_{2+x}
3. The calculated transition temperatures in the stoichiometric and hypostoichiometric oxide vary as a function of x in fairly good agreement with the experimental observation.

These results confirm that point defect formation in UO_2, even at high temperatures and in the presence of strong defect interactions, can be suitably described by mean-field ionic models, i.e. with internal polarization that can be calculated from the macroscopic dielectric properties.

2) Electronic Defects

An immediate question arising from the above considerations deals with the high temperature electronic properties. In fact, UO_2 is an insulator, its electrical conductivity being due to formation of mobile (hopping) defects. The ionic model applied above entails that the electronic defects (extranumerary electrons and holes) are strictly localized, that is to say, extra electrons and holes are associated to local lattice relaxations. Actually, it has been demonstrated [7] that the simplest mechanisms of electronic defect formation, due to the disproportioning reaction:

$$2U^{4+} \rightarrow U^{3+} + U^{5+} \qquad (4)$$

leads to the creation of local lattice strains forming "small polarons", hence extra electrons (associated with U^{+3}) and holes (associated with U^{+5}) have the same mobility and are both migrating by thermal activation.

The disproportioning reaction eq.(4) has not only formal, but also physical analogies with the *Frenkel* pair formation described by reaction (1): since electron/hole pairs are subjected to the same mean Coulombic field as the oxygen *Frenkel* pairs, their formation mechanism is expected to be governed by a free energy of formation analogous to eq.(2), i.e. containing a screening term increasing with the defect concentration, which, potentially, could involve an insulator-metal transition at a critical temperature, analogous to the above mentioned anion order/disorder transition. Actually, the experiment shows that in UO_2 the high temperature d.c. conductivity, $\sigma(T)$, exhibits marked deviations from the typical exponential dependence of single-energy activated processes (Fig.4), however, the increase in σ with temperature appears to be continuous, although the experimental measurements show a significantly larger scatter above 2500 K. Therefore, contrary to the behavior of *Frenkel* defects in UO_{2-x}, the electronic thermal defect formation does *not* display a critical insulator-metal transition.

The electronic defect interaction was calculated using an intersite screened potential [8], where the screening factor was obtained from the empirical dielectric constant (the same used for calculation of the *Frenkel* defects interaction). The intraside potential was eval-

uated from low temperature conductivity data, where the defect interaction is negligible. The results of the model calculation are shown as full lines in Fig.4 and in Fig.5. The theoretical small polaron concentration shows a clear non-vertical inflection at a temperature near to the λ-transition, which indicates the approaching of saturation in the disproportioning reaction. Furthermore, it can be seen that, due to the decrease in defect internal energy at high defect concentrations, the calculated contribution of small polarons to the heat capacity (Fig.5) is relatively small compared to that of oxygen defects.

3) Heat Capacity of the Liquid

The experimental measurements of the heat capacity in liquid UO_2 [1] show that C_p sharply decreases from 640 *J/KgK* near the solidus down to 450 *J/KgK* at a temperature just above the liquidus. A further, smoother decrease of C_p with T is observed up to approximately 4500 K.

Two important conclusions can be drawn. First, the contributions due to lattice and electronic defects tend to vanish on melting: this entails that the liquid maintain the insulator property of the solid.

Second, at higher temperatures the heat capacity decreases to approximately the value 9R (277 *J/KgK*), which corresponds to the heat capacity of a three-atomic lattice composed of ideal harmonic oscillators. This feature, which is typical for several molecular liquids (e.g. H_2O) indicates that the cohesive forces are able to sustain both *longitudinal*, and also *transversal* vibrations.

These remarks have some implications in the following discussion on the liquid thermal conductivity.

The increase of C_p with temperature above 5000 K can be fitted by an Arrehnius plot with an activation energy of approximately *3 to 4 eV*. This indicates the existence of a *6 to 8 eV* energy gap across which excitations opccur at these temperatures. Comparing this datum with the energy levels of solid urania (measured at room temperature) and with the calculated energy levels of the UO_2 molecule (Fig. 6), reveals that a gap of this magnitude exists between the 2p valence band (predominantly affected by oxygen) and the e_g subband (predominantly affected by uranium). Though this scheme pertains to low temperature configurations, and, therefore, can only be indicative for the high temperature states, we may nevertheless infer that above 5000 K the molecular bonding in the condensed phase is strongly affected by temperature. Actually, at 8200 K, the maximum temperature experimentally attained with the condensed phase, a dramatic increase in fluidity was observed, making it impossible to achieve higher temperatures [1]. This may indicate approaching of the critical point: in fact, the theoretically predicted critical temperature of UO_2 reported in the literature ranges from 6000 K to 10.000 K. The recent experiments indicate that its real value is probably not far above 8200 K.

4) Energy transport

For a long time in the past, the large discrepancy between the various measurements of the thermal conductivity k, of liquid UO_2 (Fig.7) has represented an insoluble difficulty [9] [10] [11] [12][13]. It can be seen that the measured conductivities range from the lowest value of 2.5 W/mK, measured at JRC-ITU, to the value of 5.5 W/mK (re-assessed from the initially published [9]highest value of 11 W/mK).

The recent experimental determination of the heat capacity of this material at temperatures from 2500 K to above the melting point, makes it possible to evaluate the heat diffusivity, α, in this temperature range and by discussing the dependence of α on temperature obtain new information on the conductivity above the melting point.

The thermal conductivity experimental data in solid UO_2 at temperatures above 2000 K were critically analyzed, and different interpolating functions have proposed whose values agree within 10-15%. For comparison, two sets of values of k have been adopted to calculate α in the solid: those from the MATPRO databank [17] and those used at ITU [18]. These have been plotted in Fig.8. α can be obtained by the defining relation:

$$\alpha = \frac{k}{\rho C_p} \qquad \text{where } \rho = \textit{density} \tag{5}$$

The heat diffusivity obtained from the experimentally measured k, C_p and ρ is plotted in Fig.8. In addition, the value of $k_{liq.}$ obtained at ITU (the lowest one of those reported above), and its corresponding value of $\alpha_{liq.}$ are also indicated.

Two features immediately catch our attention:

First, the liquid diffusivity value calculated from ITU data is on the extrapolated line of the solid, while the other measurements reported in Fig.8 would be at least two time larger and hence indicating a substantial discontinuity of both k and α across the melting point.

Second, the diffusivity curve in the solid is split into two segments respectively decreasing and increasing with temperature, separated by a "pit" corresponding to the λ –transition, which, being formally similar to a thermodynamical critical point, entails that $\alpha \rightarrow 0$ for $T \rightarrow T_c$.

Some general remarks enable us to interpret these features. In fact, diffusivity in crystals decreases with temperature due to increasing anharmonic vibrations (caused by lattice strains, impurities and defects): in this sense the regular decrease of α in UO_2 between RT and 2500 K can be qualitatively explained. By approaching the λ –transition the number of phonon scattering centers dramatically increases. The zero of the dynamic quantity

α at $T_t = 2670K$ is attributable to the slowness to which fluctuations decay at the critical point.

Above the λ –transition, in the oxygen sublattice the concentration of *Frenkel* pairs approaches 0.2 [16], hence the lattice displays a high degree of disorder.

Making comparisons between thermal diffusivity of crystalline and glassy forms of the same substance, we realize that the dependence on temperature is opposite in the two cases, k in the glassy phase displaying an increase with rising temperature (a typical example is provided by crystalline and fused SiO_2).

Furthermore, an analogous behavior of $\alpha(T)$ is also observed in systems where electrons carry a significant part of the heat current: in fact, in a number of metals and binary alloys undergoing magnetic λ –transitions around the *Curie* point (e.g. *Fe, Ni, Co*), a sharp minimum, located at the transition temperature, defines two branches of the curve $\alpha = \alpha(T)$ respectively descending (ordered) and ascending (disordered phase) with increasing T.

On the other hand, in systems which do not exhibit pre-melting order/disorder transitions, the reversal of the slope of $\alpha(T)$ normally occurs at the melting point. Furthermore, these materials often exhibit a discontinuity (in several cases a significant drop) in thermal diffusivity at T_m (e.g. Alkali metals, *Cu, Au*), whereas in those which previously undergo a premelting order/disorder transition the thermal diffusivity mostly increases continuously across the melting point.

Some conclusions can be drawn concerning the observed behaviour of $\alpha(T)$ in UO_2 at temperatures above the λ –transition. Actually, this transition appears to be an important discriminating feature for several physical properties, which, in the interval between T_c and T_m, are affected by the anion-sublattice disorder to an extent which has not been fully appreciated[2] . It is therefore not surprising that thermal diffusivity is so much affected by oxygen lattice defects that under conditions of pronounced oxygen disorder created by the λ –transition this quantity exhibits a temperature dependence which is typical for most glassy structures, whose passage from solid to liquid state occurs without solution of continuity in their dynamical properties. *In this context, the thermal diffusivity value obtained at ITU is conform with the observed behaviour of a set of analogous solid and fluid systems and, therefore, appears to be the correct one.*

CONCLUSIONS

The new results summarized above enable us to obtain a clearer insight into the high temperature properties of UO_2.

---

2 For instance, there is experimental evidence that in UO_2 also cation mass transport coefficients and mechanical properties are affected by the λ –transition [19].

Major uncertainties concerning the molten core response to neutron reactivity excursions have been removed by the recent experimental determination of the liquid heat capacity. The results show that the heat capacity of UO_2 falls by nearly a factor of two above the melting point, whilst in the previous reactor accident calculations the value of C_p in the liquid was tentatively assumed to be equal to the value of the solidus. This entails that the thermal response of the core is prompter and disassembly can be reached with less deposited energy, with a more favourable prognosis of the reactor accident consequences.

The problem of the extrapolation of the equilibrium partial pressure up to the critical point can be now approached by using a more realistic database of the enthalpy of the condensed phase. However, important questions on the state of gas phase are still unanswered. The first one concerns the concentration of the various molecular species under representative (transient) evaporation conditions (not-congruent or forced-congruent). The second question deals with the increasing ionization of the gas molecules at temperatures above 5000 K, which, at higher temperatures, may lead to plasma formation, entailing a further complication of the equation of state of the gas mixture. Work on this subject is starting in the frame of an international project promoted by the European Commission [20].

A final remark concerns the microscopic description of the uranium dioxide thermodynamic behavior at high temperature, and the self-consistency of the analysis of different thermophysical properties; substantial advances have been obtained by the application of mean-field *Debye-Hückel* models to the description defect formation. Concepts such as cooperative formation of sublattice disorder and pre-melting transitions cast new light on the features of the heat capacity and thermal conductivity in $UO_{2\pm x}$ above 2500 K.

One of the great merits of the microscopic analysis is to recognize the heat exchange mechanisms operating at the different temperatures (see Table I). Although the prediction of the various contributions to C_p in the vicinity of the λ –transition still presents some deviations from the experimental values, the adopted models provide on the whole a convincing physical description of the stoichiometric and off-stoichiometric uranium dioxide.

CAPTIONS OF THE FIGURES

1. Experimental measurements of the heat capacity of UO_2.
2. Experimental observation of the λ –transition in UO_{2-x} by thermal arrest during cooling after a laser-heating shot. The transition is observed as a plateau on the cooling curve. In the hypostoichiometric oxide (a) undercooling indicates the presence of a first-order transition. In the hyperstoichiometric oxide (b) the transition disappears as the cooling curve does not display any inflection.
3. Calculated heat capacity in hypostoichiometric UO_{2-x} (a) and corresponding oxygen *Frenkel* pair concentration as functions of temperature. The predicted transition in UO_{2-x} is of first order (the defect concentration curves are actual step-functions) and the transition temperature increases with x.

   (b): In the hyperstoichiometric oxide, UO_{2+x}, the transition gradually disappears with increasing x (the defect concentration curves are continuous in T).
4. Experimental and theoretical electrical conductivity in UO_2.
5. Calculated small-polaron concentration and heat capacity contribution.
6. Electronic states in UO_2 The excitation of the electrons of the *2p*-band is likely responsible for the upswing of C_p between 5000 K and 8000 K.
7. Measured thermal conductivity of UO_2.
8. Thermal diffusivity of UO_2.

REFERENCES

[1] C.RONCHI,J.P.HIERNAUT,R.SELFSLAG, G.J.HYLAND, Nucl. Sc. & Eng. 113 (1993) 1

[2] J.P.HIERNAUT,G.J.HYLAND,C.RONCHI, Int. Journ. of Thermophys. 14,2 (1993) 259

[3] M.A.BREDIG, Oak Ridge Nat. Laboratory, US Report 4437 (1969) 103

[4] P.BROWNING, G.J.HYLAND, J.RALPH, High Temp.- High Press. 15 (1983) 169-178

[5] M.T.HUTCHINGS, Journ. Chem. Soc. Faraday Trans. II 83(1987) 1083

[6] J.L.BATES et al., J. Amer. Ceram. Soc. 50 (1967) 652

[7] G.J.HYLAND, J.RALPH, High Temp.-High Press. 15 (1983) 179-190

[8] E.J.YOFFA, D.ADLER Phys. Rev. B 20,10 (1979) 4044

[9] C.S.KIM, R.A.HALEY, J.FISCHER, M.G.CHASANOV, L.LEIBOWITZ, Proceedings 7th Symposium on Thermophysical Properties, A.Cezairliyan Editor (New York, American Soc. of Mechanical Engineers) 1977, p.338-343

[10] C.OTTER, D.DAMIEN, High Temperatures-High Pressures 16 (1984) 1-6

[11] H.A.TASMAN, D.PEL, J.RICHTER, H.E.SCHMIDT, High Temperatures-High Pressures 15 (1983) 419-431

[12] J.K.FINK, L.LEIBOWITZ, High Temperatures-High Pressures 17 (1984) 17-26

[13] H.A.TASMAN, "Thermal Conductivity of Liquid UO_2", in Annual Report 1988 (TUAR88) , Commission of the European Communities, Joint Research Centre, Karlsruhe, Germany

[14] C. OTTER, J.VANDEVELDE, Rev. Int. Hautes Temp. Refr. Fr. 19 (1982) 41-53

[15] C. RONCHI, C SARI, Journ. Nucl. Mater. 50 (1974) 91-97

[16] C.RONCHI, G.J.HYLAND, Journ. of Alloys & Comp., in print (1994)

[17] O.L.HAGRMAN, Report EG&G-CDAP 3029, US Department of Energy, Idaho Operation Office, Idaho National Engineering Laboratory (1979).

[18] G.J.HYLAND, Journ. of Nucl. Mater. 113 (1983) 125

[19] Hj.MATZKE, Adv. Ceram. 17 (1986) 1-54

[20] EUROPEAN COMMISSION, INTAS Project 93-66, "Equation of State of Nuclear Fuel", Bruxelles (1994)

THEORETICAL CONTRIBUTIONS TO HEAT CAPACITY AND EXPERIMENTAL MEASUREMENTS IN UO_{2-x} (J/mole.K)

Temp.(K)	1 Harmonic	2 Anharm.	3 Crystal Field	4 Frenkel x=0.02	5 Small Polarons	6 Schottky	1 to 6 Summed x=0.02	Exp.
1000	74.8	2.5	6.0	.	.	.	83.3	84.0
1200	74.8	4.8	6.0	.	0.1	.	85.7	86.0
1400	74.8	6.9	6.0	0.0	0.2	.	87.9	88.0
1600	74.8	8.9	6.0	0.0	0.7	.	90.4	90.0
1800	74.8	10.9	6.0	0.4	1.7	.	93.8	93.0
2000	74.8	12.9	6.0	2.6	3.8	.	100.1	99.0
2200	74.8	14.8	6.0	13.6	7.1	.	116.3	109.0
2400	74.8	16.8	6.0	44.1	11.7	0.8	154.2	119.0
2600	74.8	18.8	7.0	132.4	14.8	1.2	249.1	200.0
2670	74.8	19.5	7.0	.	14.9	1.6	.	.
2800	74.8	20.8	7.0	92.4	14.5	2.2	211.8	150.0
3000	74.8	22.8	7.0	20.0	12.6	3.6	140.7	155.0
3100	74.8	23.8	7.0	12.5	11.5	4.4	134.0	161.0

TABLE I

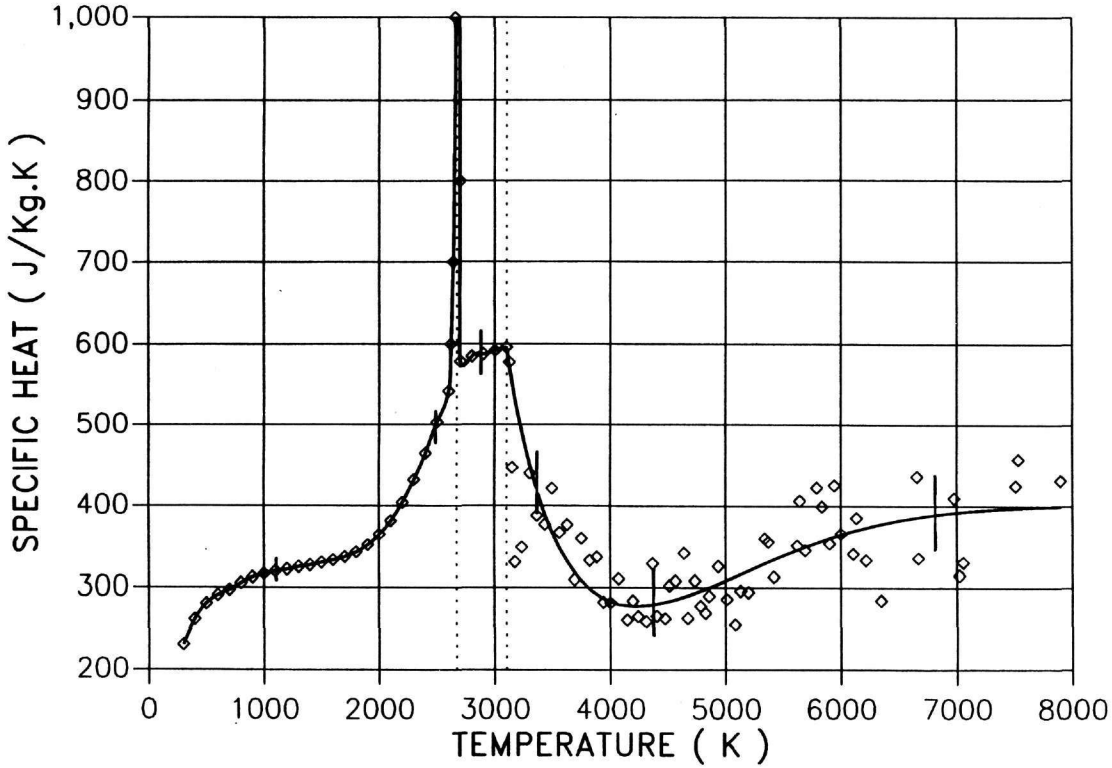
1,000
900
800
700
600
500
400
300
200
SPECIFIC HEAT (J/Kg.K)
0
1000
2000
3000
4000
5000
6000
7000
8000
TEMPERATURE (K)

FIG.1

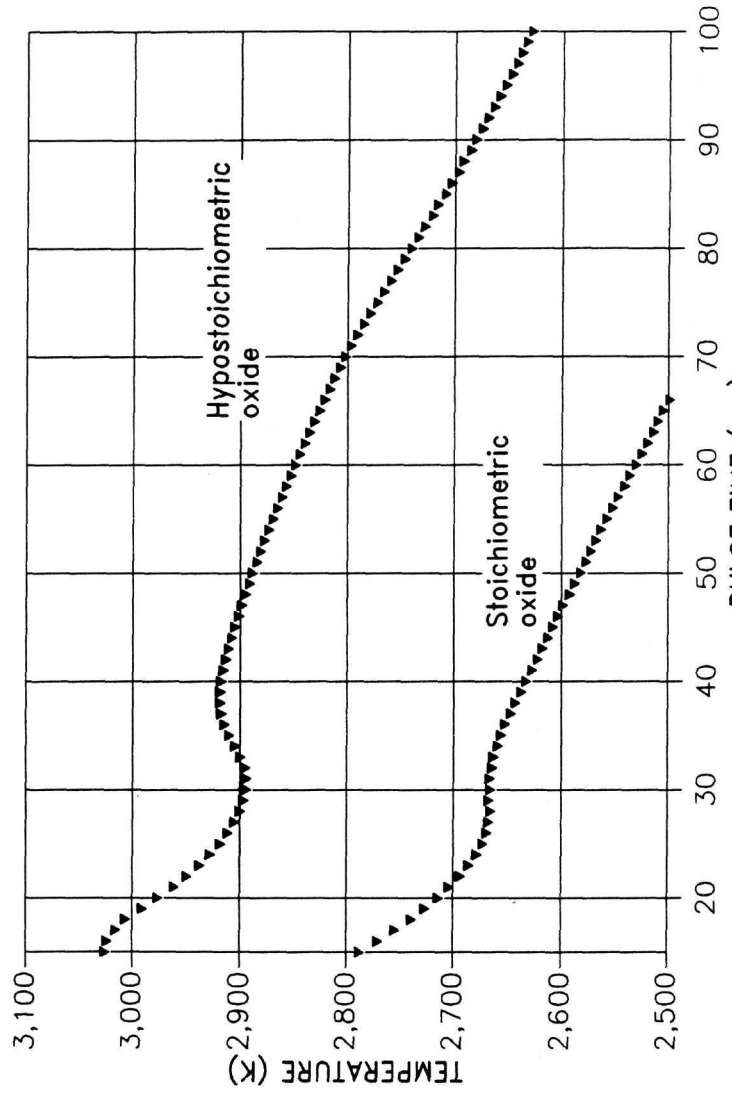
TEMPERATURE (K)
3,100
3,000
2,900
2,800
2,700
2,600
2,500
20
30
40
50
60
70
80
90
100
PULSE TIME (ms)
Hypostoichiometric oxide
Stoichiometric oxide

FIG.2a

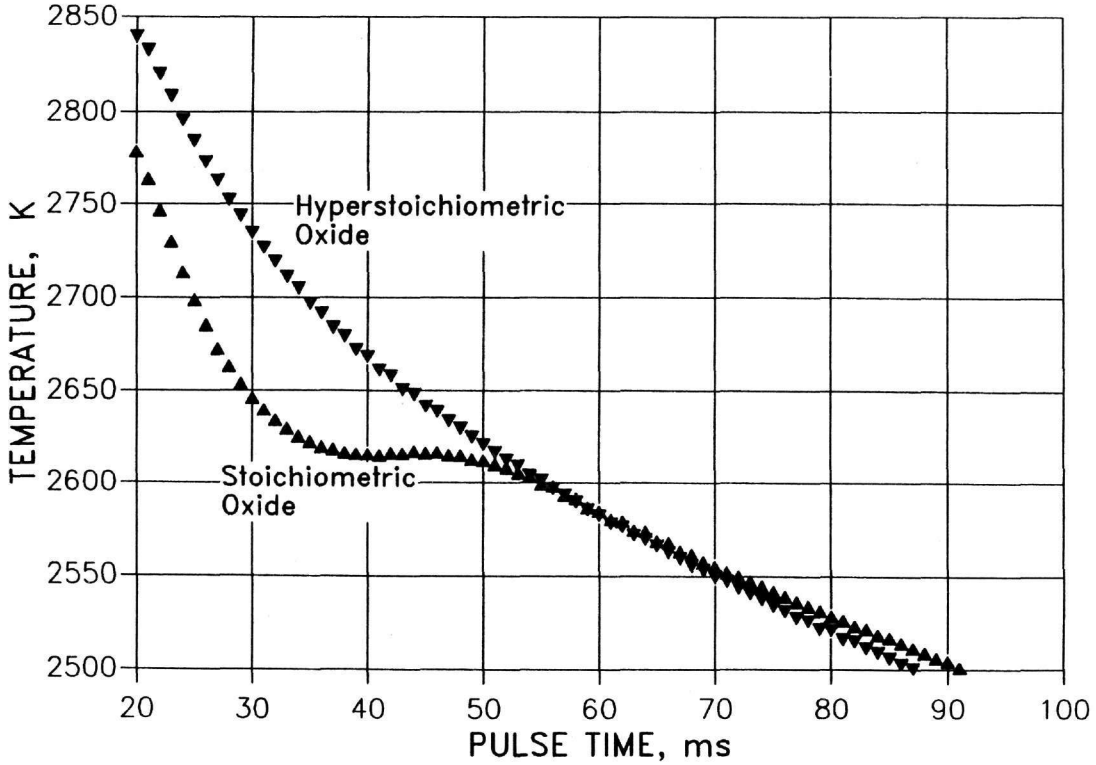
2850
2800
2750
2700
2650
2600
2550
2500
TEMPERATURE, K
Hyperstoichiometric
Oxide
Stoichiometric
Oxide
20
30
40
50
60
70
80
90
100
PULSE TIME, ms

FIG. 2b

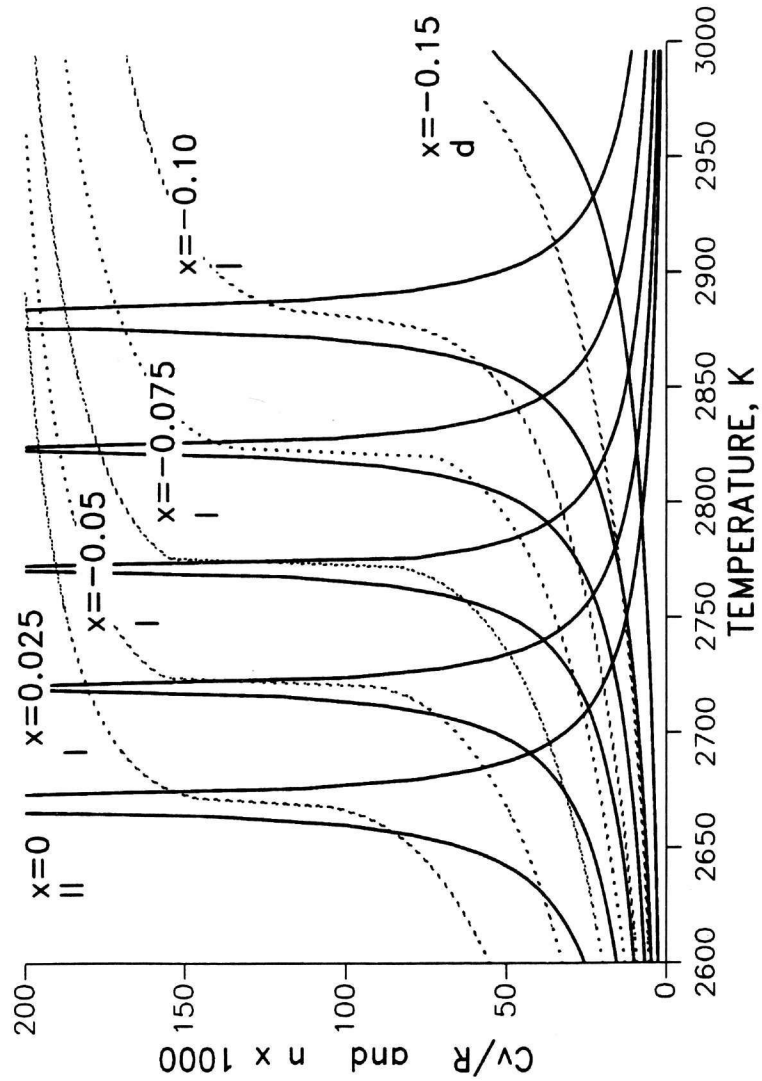
x=0
x=0.025
x=−0.05
x=−0.075
x=−0.10
x=−0.15
d
Cv/R and n x 1000
TEMPERATURE, K
200
150
100
50
0
2600
2650
2700
2750
2800
2850
2900
2950
3000

FIG.3a

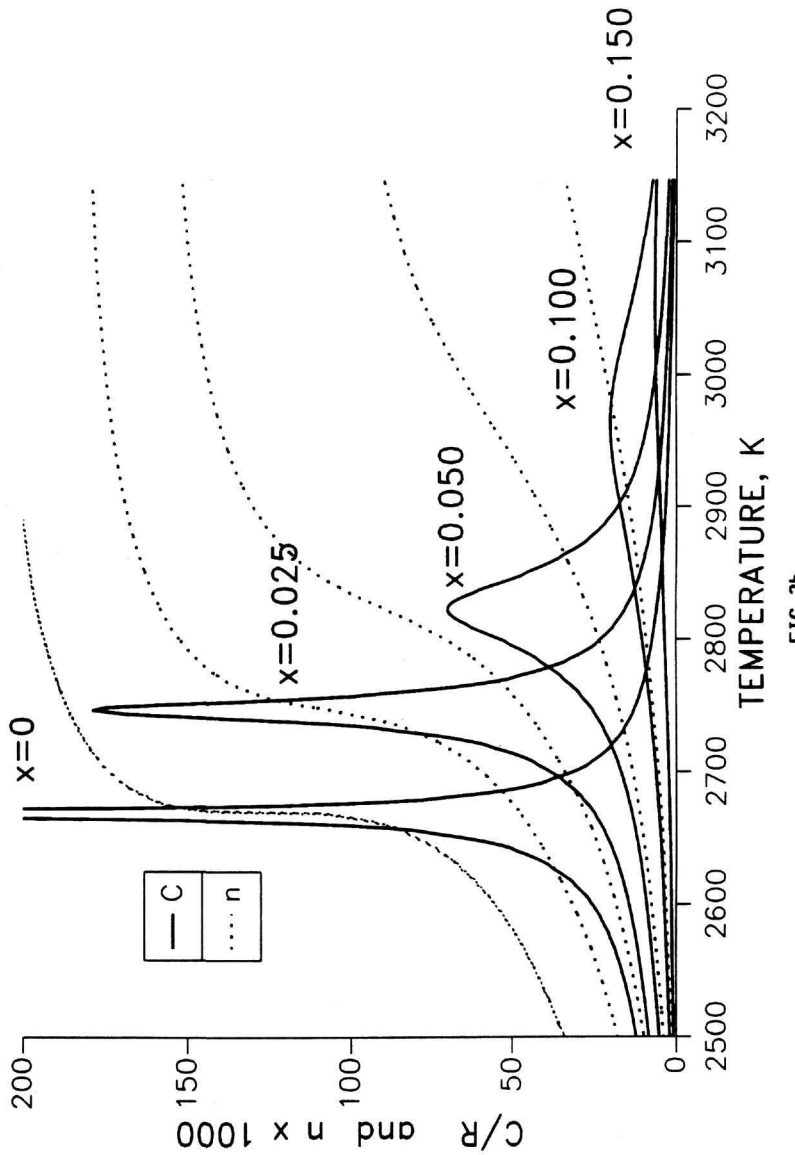
C/R and n x 1000
200
150
100
50
0
2500
2600
2700
2800
2900
3000
3100
3200
TEMPERATURE, K
C
n
x=0
x=0.025
x=0.050
x=0.100
x=0.150

FIG.3b

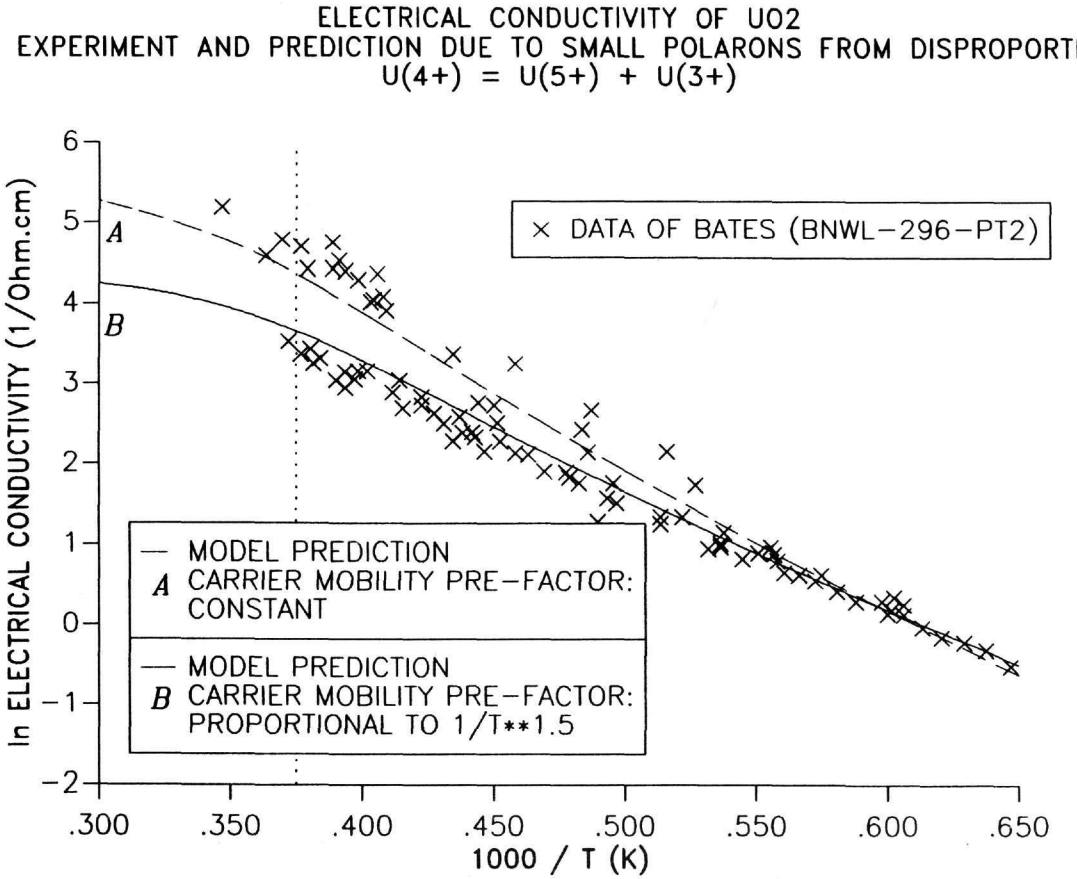
ELECTRICAL CONDUCTIVITY OF UO2
EXPERIMENT AND PREDICTION DUE TO SMALL POLARONS FROM DISPROPORTION
U(4+) = U(5+) + U(3+)
× DATA OF BATES (BNWL−296−PT2)
A
B
— MODEL PREDICTION
A CARRIER MOBILITY PRE−FACTOR:
CONSTANT
— MODEL PREDICTION
B CARRIER MOBILITY PRE−FACTOR:
PROPORTIONAL TO 1/T**1.5
ln ELECTRICAL CONDUCTIVITY (1/Ohm.cm)
6
5
4
3
2
1
0
−1
−2
.300
.350
.400
.450
.500
.550
.600
.650
1000 / T (K)

FIG.4

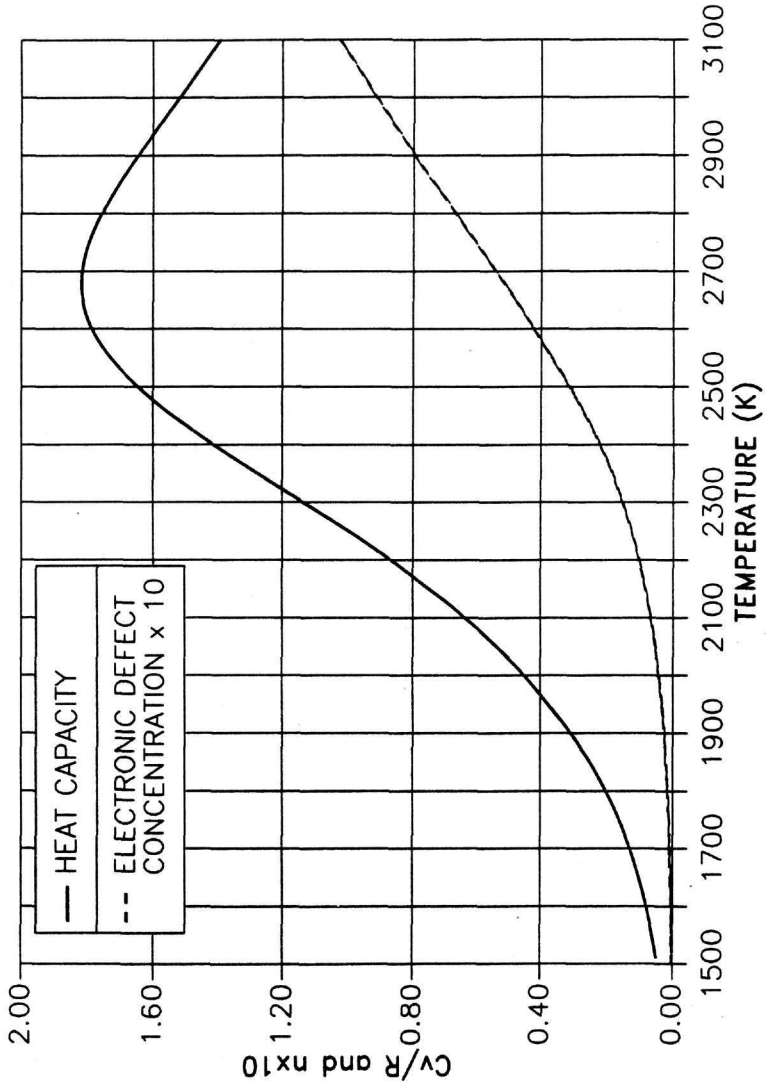
HEAT CAPACITY
ELECTRONIC DEFECT CONCENTRATION x 10
Cv/R and nx10
TEMPERATURE (K)
2.00
1.60
1.20
0.80
0.40
0.00
1500
1700
1900
2100
2300
2500
2700
2900
3100

FIG. 5

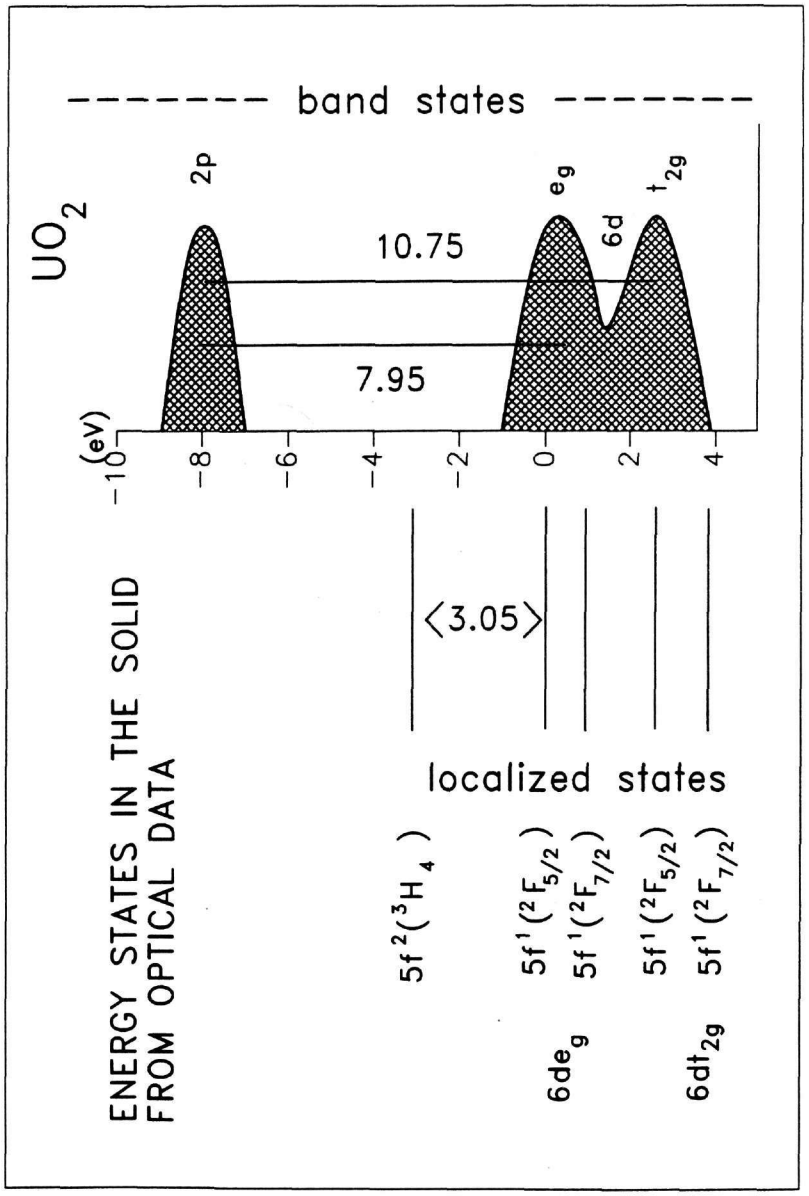
band states
UO_2
2p
e_g
t_{2g}
6d
10.75
7.95
(eV)
−10
−8
−6
−4
−2
0
2
4
⟨3.05⟩
localized states
$5f^2(^3H_4)$
$5f^1(^2F_{5/2})$
$5f^1(^2F_{7/2})$
$6de_g$
$5f^1(^2F_{5/2})$
$5f^1(^2F_{7/2})$
$6dt_{2g}$
ENERGY STATES IN THE SOLID
FROM OPTICAL DATA

FIG. 6

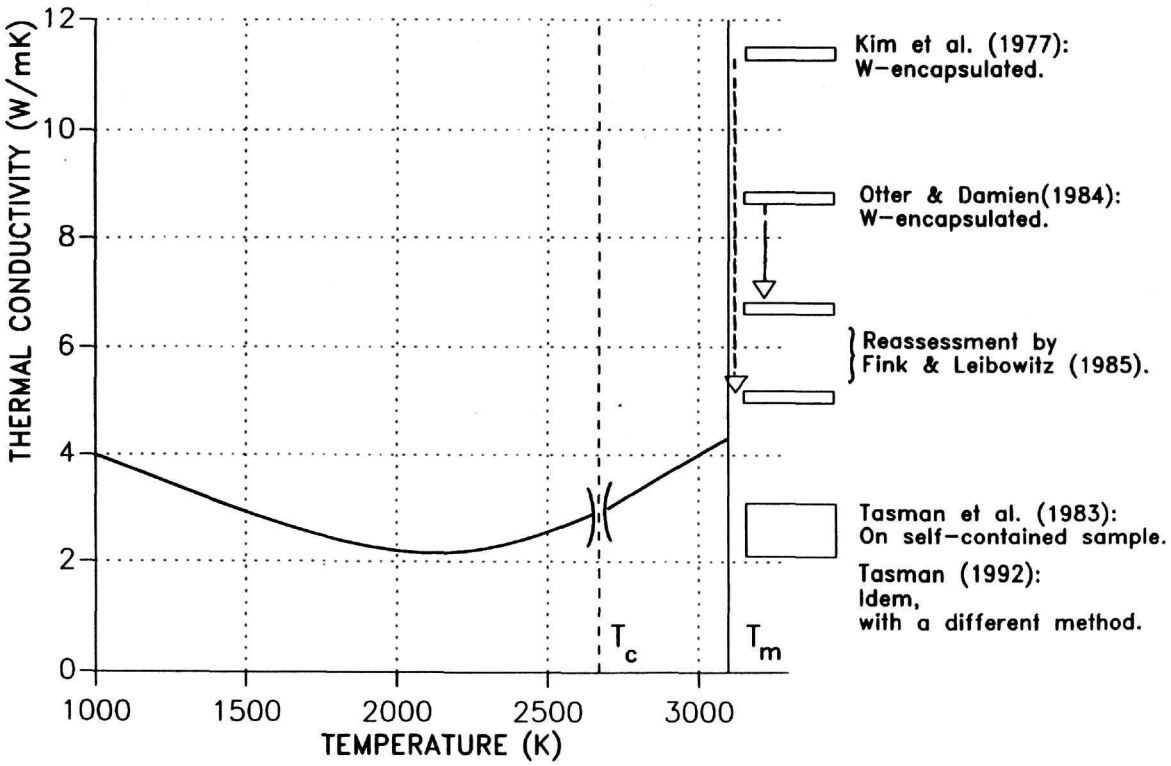
THERMAL CONDUCTIVITY (W/mK)
12
10
8
6
4
2
0
1000
1500
2000
2500
3000
TEMPERATURE (K)
T_c
T_m
Kim et al. (1977):
W-encapsulated.
Otter & Damien(1984):
W-encapsulated.
Reassessment by
Fink & Leibowitz (1985).
Tasman et al. (1983):
On self-contained sample.
Tasman (1992):
Idem,
with a different method.

FIG. 7

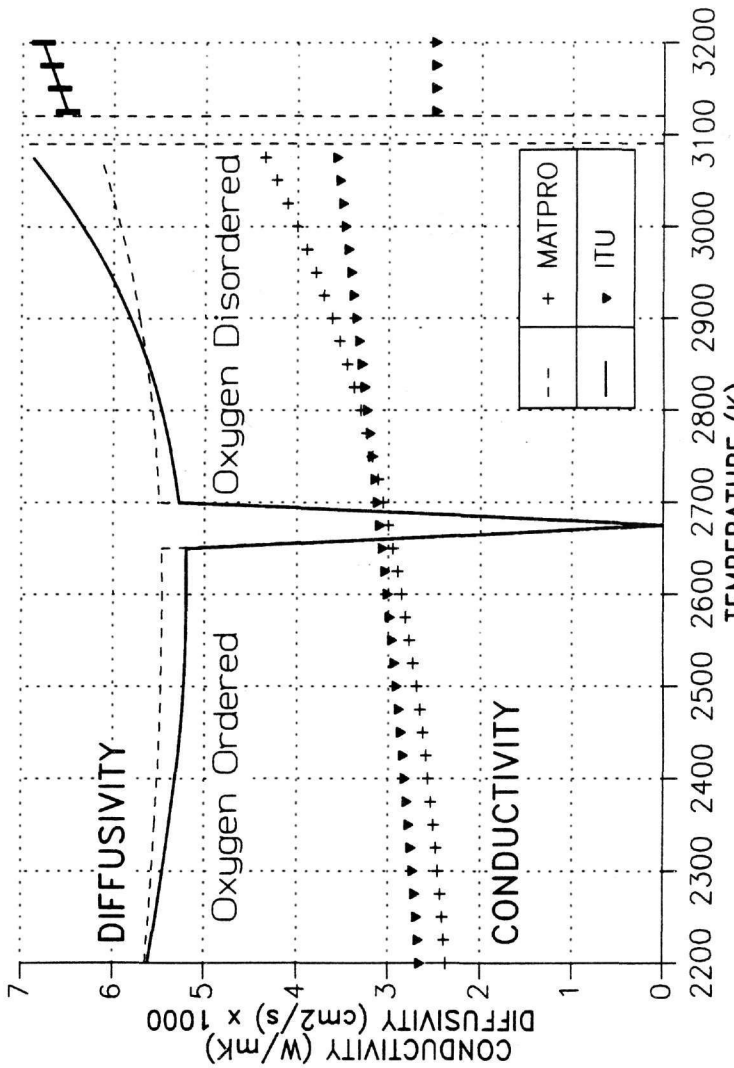
DIFFUSIVITY
Oxygen Ordered
Oxygen Disordered
CONDUCTIVITY
+ MATPRO
ITU
CONDUCTIVITY (W/mK)
DIFFUSIVITY (cm2/s) x 1000
TEMPERATURE (K)
0
1
2
3
4
5
6
7
2200 2300 2400 2500 2600 2700 2800 2900 3000 3100 3200

FIG. 8